Clays and Clay Minerals, Vol. 39, No. 5, 531–539, 1991.

STRUCTURE-COMPOSITION RELATIONSHIPS IN TRIOCTAHEDRAL CHLORITES: A VIBRATIONAL SPECTROSCOPY STUDY

A. C. PRIETO,[1] J. DUBESSY,[2] AND M. CATHELINEAU[2]

[1] Departamento de Fisica de la Materia Condensada, Cristalografia y Mineralogia
Universidad de Valladolid, 47011, Valladolid, Spain

[2] CREGU and GS CNRS-CREGU, BP 23, 54501
Vandoeuvre les Nancy Cedex, France

Abstract—Raman and Fourier-transformed infrared spectra of natural trioctahedral chlorites of polytype IIb were obtained for a series of samples characterized by distinct Fe/(Fe + Mg) and Si/Al ratios ranging, respectively, from 0.04 to 0.94 and from 5.18 to 1.86. All samples were characterized by X-ray powder diffraction, and quantitative electron microprobe analysis. In the 3683–3610-cm^{-1} spectral range, the wave number of the OH-stretching band from the 2:1 layer (band I) decreased with an increase of iron content at constant Al(IV) content. The more intense bands II and III at about 3600 cm^{-1} and 3500 cm^{-1}, were assigned to hydroxyl groups involved in hydrogen bonds: (SiSi)O . . . HO, with the hydrogen bonds being roughly perpendicular to the basal plane, and (SiAl)O . . . HO, respectively. At higher tetrahedral Al and octahedral Fe contents, spectra exhibited OH-bands II and III, respectively, at a lower frequency. Band III intensity increased and band II was enlarged for chlorites displaying higher Al(IV) contents.

In the 1300–1350-cm^{-1} spectral range, most infrared spectra displayed intense bands at 1090, 1050, 990, and 960 cm^{-1}, which were assigned to T–O stretching of symmetry species A1 and E1. The second type of bands observed both in Raman and infrared spectra were at about 650–800 cm^{-1}; they were assigned to OH vibrations and were strongly dependent on the composition of the interlayer octahedral sheet, especially on the Fe content.

Key Words—Chlorite, Hydroxyl, Infrared spectroscopy, Raman spectroscopy, Structure.

INTRODUCTION

Chlorites are ubiquitous phyllosilicates found in sedimentary, metamorphic, and hydrothermal environments. Their chemical compositions, especially the Si/Al and Fe/(Fe + Mg) ratios, are a function of the physical-chemical conditions of crystallization (Cathelineau and Nieva, 1985; Walshe, 1986; Cathelineau, 1988; Chernovsky *et al.*, 1988; Laird, 1988). Trioctahedral chlorites have been poorly studied by spectroscopic techniques. Most of the available data concern infrared (IR) absorption spectroscopy, and some correlations between vibrational bands and chemical composition have been made (Tuddenham and Lyon, 1959; Stubican and Roy, 1961; Hayashi and Oinuma, 1965; Oinuma and Hayashi, 1968; Farmer, 1974; Shirozu and Nomoi, 1972; Shirozu *et al.*, 1975; Shirozu, 1980, 1985). Most of these studies, however, are not complete and fail to take into account all solid solutions. In addition, no studies have been made by Raman spectroscopy. The interpretation and assignment of the different spectral bands has been based on the general model of phyllosilicates defined from IR spectra (Farmer, 1974; Ishii *et al.*, 1967). Indeed, the poor knowledge of symmetry sites and of molecular groups in single crystals does not allow the accurate use of the molecular hypothesis (Poulet and Mathieu, 1970). Vibrational modes of the crystal, however, can be assigned to a first approximation to fundamental vibrations of tetrahedral and octahedral units and OH-groups.

The aim of this paper is to report basic Raman spectroscopic data of these minerals and to depict changes occurring in the spectra as a function of the Si-Al and Fe-Mg substitutions. Such Raman data will help in the use of micro-Raman techniques for quick characterization of trioctahedral chlorites at the micrometer scale. Such a technique will be useful for the study of small crystals, which are common in sedimentary and diagenetic environments.

EXPERIMENTAL

X-ray powder diffraction (XRD) patterns were made on a SIGMA 2080 instrument (Jobin Yvon) using CuKα radiation on powders and orientated crystals. Chemical compositions were determined with a CAMEBAX automatic electron microprobe at Nancy I University using the following analytical conditions: 15-kV acceleration voltage, 6-s counting time, 6-nA excitation current; correction program ZAF Cor 2. The following minerals were used as standards: corundum (Al), albite (Na, Si), hematite (Fe), apatite (Ca), orthoclase (K), forsterite (Mg), rutile (Ti), and rhodonite (Mn). The maximum analytical error was 3% of the total.

IR spectra were recorded on a Mattson Cygnus-100 FT-IR spectrometer. Samples were prepared in KBr pellets and Nujol films for the 4000–400-cm^{-1} and 80–600-cm^{-1} spectral ranges, respectively. Raman spectra were recorded on an X-Y device from DILOR company using a 700-intensified photodiode-array multichannel detector. The foremonochromator was used

Table 1. Museum collection, geological origins, structural parameters, and crystallinity of the studied chlorites.

Chlorite No.	Mg P1	Mg P2	Mg P3	Fe-Mg P4	Fe-Mg B5	Fe P6	Fe B7	Fe B8
Museum No.	P108902	P12644	P137510	P107749	B2976	P12466	B5084	B5204
Origin	Zermatt CH	Besafotra MDG	Angatsin MDG	Laifour F	Blausee CH	Evisa F	Nucice CS	Thuringen D
Museum	Paris	Paris	Paris	Paris	Bern	Paris	Bern	Bern
d(001)(Å)	14.33	14.17	14.15	14.15	14.10	14.12	14.11	14.12
b_0(Å)	9.234	9.240	9.240	9.300	9.288	9.342	9.342	9.328
Polytype	II(B)	II(B)	II(B)	II(B)	II(B)	II(B)	II(B)	II(B)
Crystallinity	M	M	M	P	M	P	P	P

M = single crystal; P = polycrystalline powder.

in the substractive mode to remove the exciting radiations; the dispersion of the different radiations resulted only from the spectrograph. The exciting radiation of 488.0 or 514.5 nm was provided by an Ar^+ laser (2020-05 model from Spectraphysics). The range of spectral resolution was about 4 cm^{-1}. Polished chlorite monocrystals (P1, P2, P3, and B5) were analyzed in the back-scattering geometry with the laser perpendicular or parallel to the (001) basal planes both in the macroscopic and microscopic modes. Spectra of cryptocrystalline samples (P4, P6, B7, and B8) were only obtained with the microscope.

SAMPLE DESCRIPTION

Eight samples were chosen for describing the Si-R^{3+} (mostly Al) tetrahedral substitution and Fe-Mg octahedral substitutions. Samples were kindly provided by the Museum National d'Histoire Naturelle de Paris (P) and the Musée d'Histoire Naturelle de Bern (B). Sample numbers from Paris and Bern Museums and their origins are given in Table 1. Samples P1, P2, P3, and B5 are well-crystallized large crystals (>1 mm), whereas samples P4, P6, B7, and B8 are small (<0.5 mm) crystal assemblages and were therefore extracted by classical techniques.

Structural parameters are given in Table 1. XRD of orientated agregates showed all samples to be polytype IIb. The structural formulae given in Table 2 were calculated on the basis of 14 oxygens. All the Si was assigned to the tetrahedral sheet, and the number of tetrahedral atoms per formula was then completed to 4 with Al. The remaining Al was assigned to the octahedral sites, along with Mg and Fe. Fe was assumed to be divalent. Major compositional features of studied chlorites are depicted (Figure 1a) in the Fe/(Fe + Mg) vs. Si diagram (Foster, 1962). The good correlation between Fe and Mg indicates that Fe and Mg substituted mutually in the R^{2+} site (Figure 1b). Therefore, the Fe^{3+} content was probably only a very small proportion of the total Fe content, which supports the assumption about the chosen Fe valence.

RESULTS AND DISCUSSION

All data are given in Table 3. Stretching vibrations of hydroxyl groups give rise to intense bands in IR and Raman spectroscopic bands in the 3400–3700-cm^{-1} spectral range (Figures 2 and 3). The spectra show significant differences of wave number, intensity, and shape with composition (Figures 2–4). Three groups of bands were identified that are characteristic of trioctahedral chlorites.

Bands in the 3683–3610-cm^{-1} spectral range

In the 3683–3610-cm^{-1} spectral range a relatively weak band (band I) was observed in the IR spectra, which was more intense in the Raman spectra. The frequency of this band was close to that found for talc

https://doi.org/10.1346/CCMN.1991.0390508 Published online by Cambridge University Press

and was assigned to the stretching of OH groups from the 2:1 layer (Serratosa and Vinas, 1964; Hayashi and Oinuma, 1965, 1967; Prieto *et al.*, 1990). The dependence of the frequency of this band on crystal chemistry is more clearly shown by the Raman spectra, in which band overlapping is less important than in IR spectra. Correlations with d(001), Al^{IV}, and Fe contents are given in Figure 4. The wavenumber of this band does not vary significantly from samples P1 to P3, all of which have the same iron content. In contrast, an increase in iron content with roughly constant Al^{IV} is accompanied by a significant decrease in wavenumber. Therefore, this band appears to be controlled mainly by the bulk iron content. The large wavenumber of this band indicates that the hydroxyl group is not involved in hydrogen bonds. As all hydroxyl groups from the interlayer are involved in hydrogen bonds, band I was therefore assigned to hydroxyl groups from the octahedral sheet (Prieto *et al.*, 1990). The intensity of band I clearly depended on the orientation of the electric field E of the laser. The spectra in Figure 5 show that the intensity of band I with E parallel to the (001) plane is higher than with E perpendicular to (001) planes. Therefore, these hydroxyl groups lie at a shallow angle close to the basal planes. The Si-Al substitution at constant iron was accompanied by the appearance of a new Raman band at 3640 cm^{-1} in sample P3 (Figure 5). It was assigned to stretching of OH bonded to octahedral Al, which compensates the charge deficit of the tetrahedral sheet. The Fe-Mg substitution at roughly constant Si-Al was accompanied by both a shift towards low frequency and a widening of the bands. These results confirm the hypothesis of Farmer (1974), that band frequency is dependent on the amount of Mg substitution.

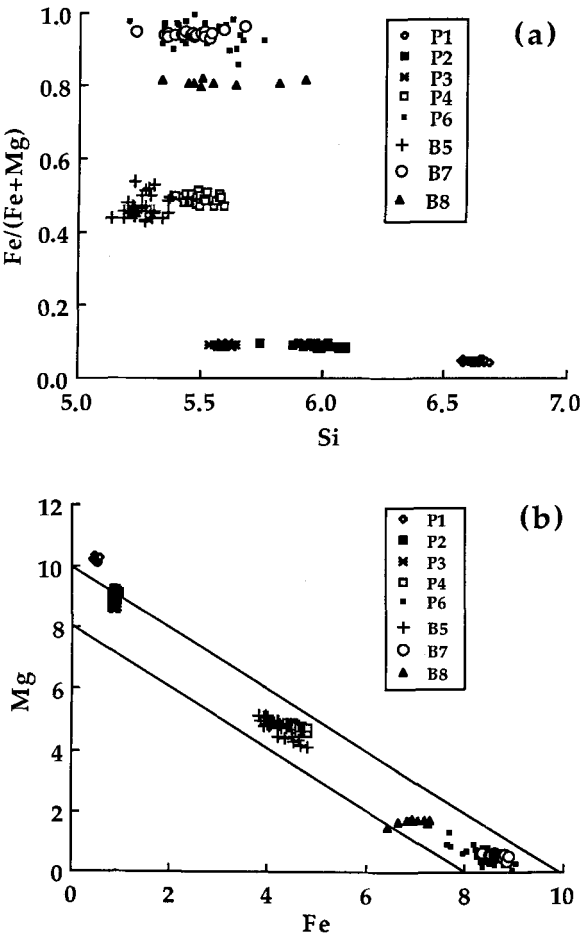

Figure 1. (a) Projection of the composition of chlorites in the Fe/(Fe + Mg)-Si plane. Compositions were determined by quantitative electron microprobe analysis. (b) Fe-Mg diagram applied to chlorite compositions determined by quantitative electron microprobe analysis.

Bands in the 3630–3380-cm^{-1} spectral range

The two bands (band II and III) were more intense and had large widths at half height (about 150–200 cm^{-1}). IR spectra showed a decrease in frequency of these bands for the Si-Al substitution at constant Fe/Mg and for the Fe-Mg substitution at constant Si/Al. Lower frequency bands, compared with band I, indicated that the corresponding hydroxyl groups were involved in hydrogen bonds. Band II was assigned to (SiSi)O . . . HO and band III to (SiAl)O . . . HO (Shirozu 1980, 1985). Z(X + Y, X + Y)Z and X + Y(Z, Z)X + Y micro-Raman spectra showed smaller inten-

Table 2. Mean structural formulae of chlorites calculated from electron microprobe analysis.

S	n	Si	Al(IV)	Al(VI)	Mg	Fe	Vac.	Fe/(Fe + Mg)	K + Na + 2Ca
P1	30	6.626	1.280	1.374	10.245	0.499	0.024	0.046	0.006
P2	27	5.998	1.969	2.002	9.128	0.884	0.020	0.088	0.004
P3	26	5.595	2.407	2.405	8.691	0.858	0.044	0.090	0.006
P4	25	5.496	2.548	2.504	4.757	4.572	0.123	0.490	0.005
B5	35	5.261	2.927	2.739	4.769	4.161	0.143	0.466	0.008
P6	25	5.501	2.791	2.499	0.509	8.382	0.318	0.943	0.037
B7	20	5.452	2.575	2.548	0.538	8.666	0.220	0.941	0.162
B8	12	5.575	3.003	2.425	1.667	6.954	0.376	0.807	0.097

S = sample; n = number of analysis; Vac. = octahedral vacancy.

https://doi.org/10.1346/CCMN.1991.0390508 Published online by Cambridge University Press

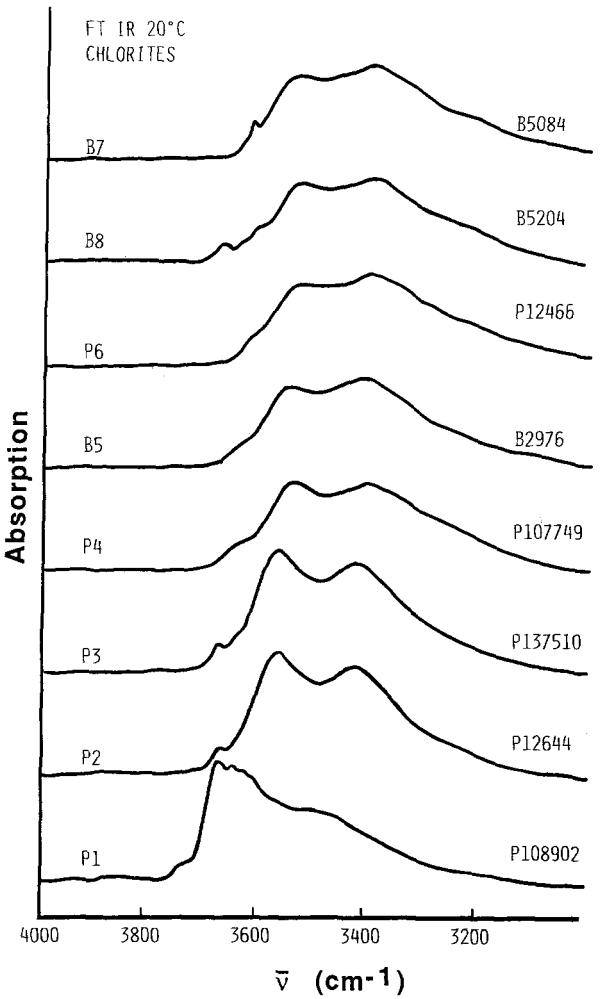

Figure 2. Infrared spectra of stretching vibrations of hydroxyl groups in the 3000–4000-cm^{-1} spectral range obtained on the chlorite series.

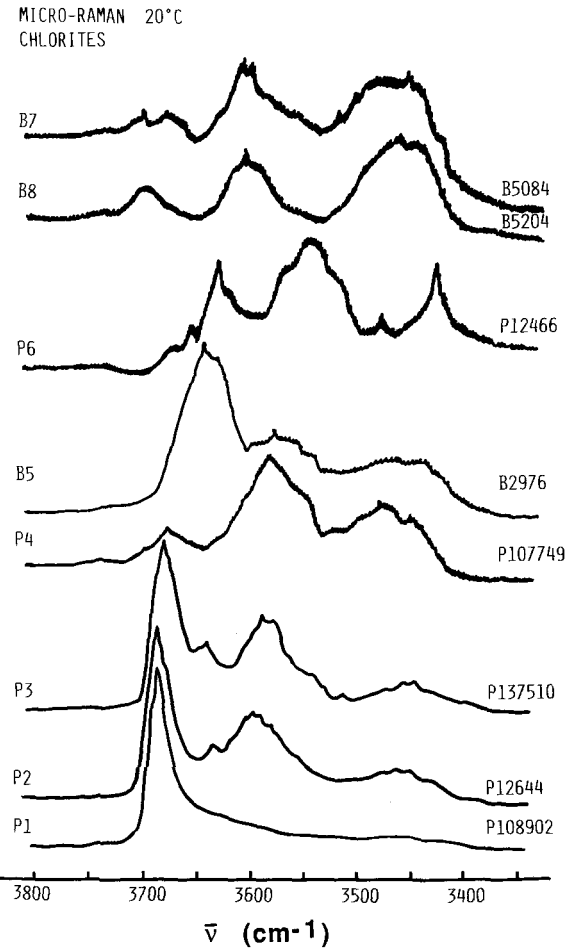

Figure 3. Micro-Raman spectra of stretching vibrations of hydroxyl groups in the 3200–3800-cm^{-1} spectral range obtained on the chlorite series.

sity of both bands II and III for the Mg-rich chlorites (samples P1, P2, and P3) than for the Fe-rich chlorites. Therefore, most of the hydrogen bonds associated with band II were roughly perpendicular to the basal plane. This was confirmed by polarization measurements on a macrosample in the back-scattering geometry (Prieto *et al.,* 1990). The increase of tetrahedral Al and octahedral Fe induced a shift of bands II and III towards low frequency with the increase of Al^{IV}. As Al^{IV} increased, the intensity of band III increased and band II became broader (Figures 2 and 4) (Hayashi and Oinuma, 1965; Farmer, 1974; Shirozu, 1980).

Bands in the 1300–50-cm^{-1} spectral range

Vibrations of the tetrahedral layer of phyllosilicates may be considered as originating in the pseudohexagonal rings (T_2O_5) of the 2:1 layer having a maximum symmetry C_{6v} (Ishii *et al.,* 1967). Normal vibrational modes of this group were assigned to the following symmetry species: $2A_1 + 3B_1 + 1B_2 + 3E_1 + 3E_2$. A_1, E_1, and E_2 are Raman active, whereas A_1 and E_1 are IR active. Frequency calculations were reported available by Ishii *et al.* (1967), Vedder (1964), and Pampuch and Ptak (1968). Substitution of Si by Al induced a loss of symmetry of T_2O_5 groups to Cs. In spite of this reduction of symmetry, the assumption of C_{6v} symmetry is convenient for the assignment of the different bands observed in both spectroscopies (Figures 6 and 7). IR spectra of all samples displayed four intense bands at 1090, 1050, 990, and 960 cm^{-1}. They were assigned to T–O stretching of symmetry species A_1 and E_1. At Fe content of <0.01, the Si substitution by Al (increase of Al^{IV}) resulted in the overlapping of the different bands into an unresolved composite band at 990 cm^{-1} (Shirozu, 1985). The bands at about 1080 cm^{-1} (samples B8 and, possibly, B7) were partly assigned to a slight quartz contamination, as shown by the doublet at about 780–798 cm^{-1}. The bands at 1040–

https://doi.org/10.1346/CCMN.1991.0390508 Published online by Cambridge University Press

Table 3. Raman data for well-crystallized chlorites.

P137510		P12644		P108902		B2976		Assignment	
⊥ (001)	∥ (001)	⊥ (001)	∥ (001)	⊥ (001)	∥ (001)	⊥ (001)	∥ (001)		
60 vw									
81 vw	78 w							$\nu_6(F_{2u})$	MO_6
92 vw								$\nu_4(F_{1u})$	MO_6
105 m	105 m			108 m	105 m			$\nu_5(F_{2g})$	MO_6
			119 w						
135 s	132 w					130 s	129 s		
						138 s	138 m	E_2^3	$\nu(T_2O_5)$
159 vw				157 vw			150 vw	$\nu_2(E_g)$	MO_6
179vw	179 vw	172 w					179 vw		
188 vw									
207 m	208 vs	202 m	203 vs	198 m	197 vs	204 m	207 m		
222 w				220 vw	228 vw	221 w	227 vw	$\nu_1(A_{1g})$	MO_6
							238 vw		
261 vw				250 vw					
							266 vw		
280 w	279 w		285 vw	286 w	287 w	281 w		E_1^3	$\nu(T_2O_5)$
	306 w	304 w	303 vw	297 vw		312 vw	292 w		
332 vw				333 vw	332 vw		335 vw		
357 s	357 m	354 s	355 m	356 s	355 w	364 m	364 m	$MO_4(OH)_2$	2:1
			371 vw		372 vw	383 vw	382 vw		
388 w	387 w	390 vw	391 vw						
				416 vw		407 vw	411 w	Skeletal modes	
429 w				427 w					
	438 vw	445 m	445 w	437 vw	442 vw				
460 w	466 w	458 vw	459 w	461 w	461 w			Librat. (OH)	
				472 vw	472 w				
	497 vw					500 vw	504 vw		
523 vw	514 vw	510 vw							
		519 vw	517 vw					E_2^2	
		530 vw		531 m		528 w			$\nu(T_2O_5)$
552 vs	550 s	548 vs	550 s	543 s	544 w	545 vs	544 vs	E_1^2	
		575 vw				574 vw			
	635 vw				614 vw		612 w		
	667 m				659 m			Librat. OH	$\nu(T_2O_5)$
682 vs	678 s	683 vs	680 vs	682 vs	680 m	667 vs	665 vs	A_1^2, E_2^1	
							669 w		
724 vw		724 vw		719 vw					
						752 vw			
775 vw	778 vw					782 m	787 m	Librat.	(SiAlO···OH)
				791 vw					
802 w	814 vw			812 vw	816 vw	809 m	809 m		
	904 vw	903 vw	906 vw	909 vw		891 vw	903 w	A_1^1	$\nu(T_2O_5)$
961 w	962 vw	951 vw		965 vw	962 w				
	986 vw	987 vw	998 vw		995 w	981 vw	986 vw		
						1019 vw	1014 vw		
							1033 vw	E_1^1	$\nu(T_2O_5)$
1047 w	1046 w	1054 m	1050 m	1057 w	1057 w		1057 w		
1078 m		1083 m		1071 w		1072 w			
				1094 w					
3450 vw						3448 vw			
						3470 vw	3462 w		(SiSi)O···OH
3540 w	3558 vw	3565 w				3542 w	3550 m	ν(OH)	
3587 m	3585 m	3592 m	3590 s			3576 m	3576 m		(SiAl)O···OH
3637 w		3636 vw		3642 w	3626 w	3641 vs	3639 vs		
		3665 w	3667 w				3669 vw	ν(OH)	2:1
3677 s	3680 w	3683 vs	3680 m	3685 vs	3681 m				
							3740 vw		

vs = very strong; s = strong; m = medium; w = weak; vw = very weak.

https://doi.org/10.1346/CCMN.1991.0390508 Published online by Cambridge University Press

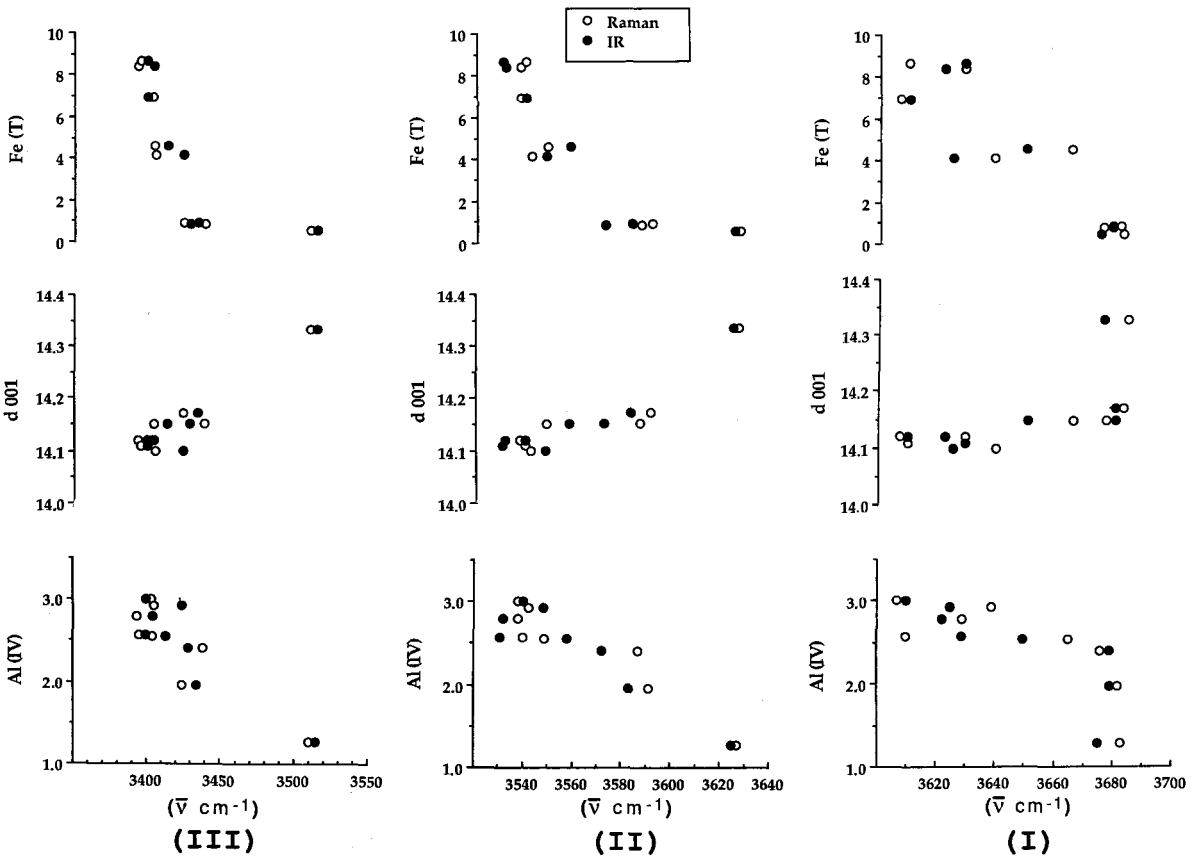

Figure 4. Correlation of d(001), bulk Fe content, and Al^{IV} with wavenumber of OH-stretching bands I, II, and III obtained on the chlorite series by Raman and infrared spectroscopy.

1090 cm^{-1} were weak in the Raman spectra. The band at 1050 cm^{-1} was strongly polarized and had a maximum intensity if the electric field of the laser was perpendicular to the basal planes [X + Y(Z, Z)X + Y]. Therefore, this band corresponds to the bonds between the apical oxygen and the tetrahedral cation. Its frequency shifted slightly towards lower values with increasing Al^{IV} (Figure 7).

The second type of band observed in both Raman and IR spectra was located at about 650–800 cm^{-1}. Hydrogen substitution by deuterium demonstrated that these bands contain a contribution of OH vibrations (Shirozu and Ishida, 1982; Shirozu, 1985): the band at about 800 cm^{-1} was assigned to one vibrational mode, and the band at 680 cm^{-1} was assigned to another vibrational mode. The intensity of the 800-cm^{-1} Raman bands increased, shifted towards higher frequency, and split into several components with an increase in the Fe content of the samples, indicating a control by octahedral substitution. Raman spectra showed no dependence on the orientation, suggesting contribution of all OH in all the orientations. IR spectra showed less intense bands in the 800 cm^{-1} region, except for sample B8, which was slightly contaminated by quartz. Quartz contamination cannot account for the Raman spectra, inasmuch as the irradiated volume was small and controlled under the optical microscope.

The intense band in both the Raman and IR spectra at about 650 cm^{-1} decreased in intensity as Al^{IV} or Fe increased. In addition, this band split into two components if Fe/(Fe + Mg) > 0.5. Therefore this vibration was strongly dependent on the composition of the interlayer octahedral sheet. It was assigned to a combination of OH vibration and movements in the tetrahedral sheet (Ishii *et al.*, 1967; Shirozu and Ishida, 1982; Shirozu, 1985).

In the 350–550-cm^{-1} region, Raman spectra exhibited well-defined bands (Figure 8), whilst our IR spectra displayed relatively poor quality features. The intensity of the band at 550 cm^{-1} was independent of the orientation in all the samples. The substitution of Si by Al or the substitution of Mg by Fe induced a slight decrease in frequency and in width at half height. It was assigned to vibrations of T_2O_5 groups of E_2^1 symmetry.

Weak Raman bands were noted between 500 and 400 cm^{-1}. Their intensity did not seem to depend on the orientation, but decreased as the Fe content in-

https://doi.org/10.1346/CCMN.1991.0390508 Published online by Cambridge University Press

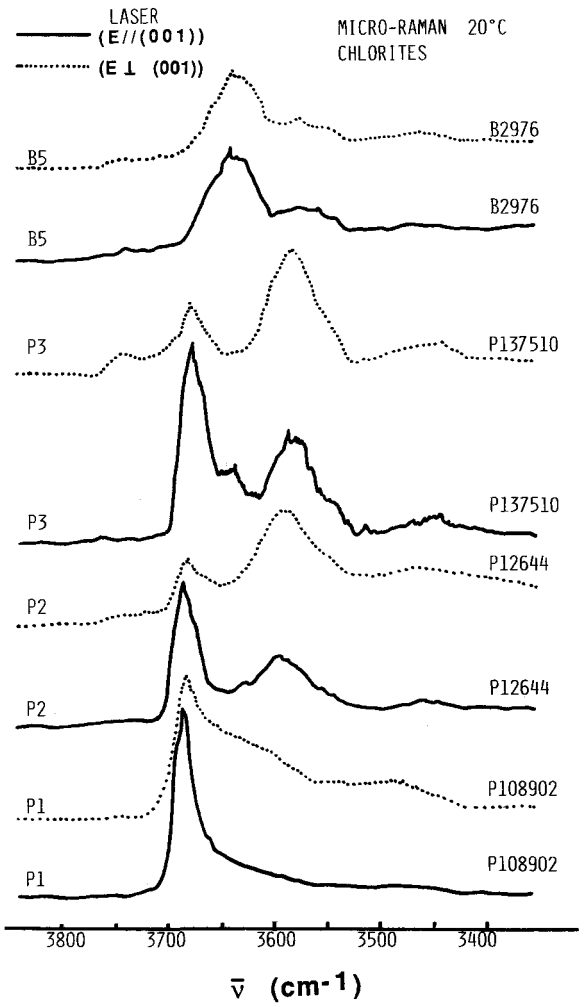

Figure 5. Different orientations of OH groups in chlorites shown by Raman spectra recorded with laser beam perpendicular to (001) planes [Z(X + Y, X + Y)Z] or parallel to (001) planes [X + Y,(Z, Z)X + Y]. (E = electric field).

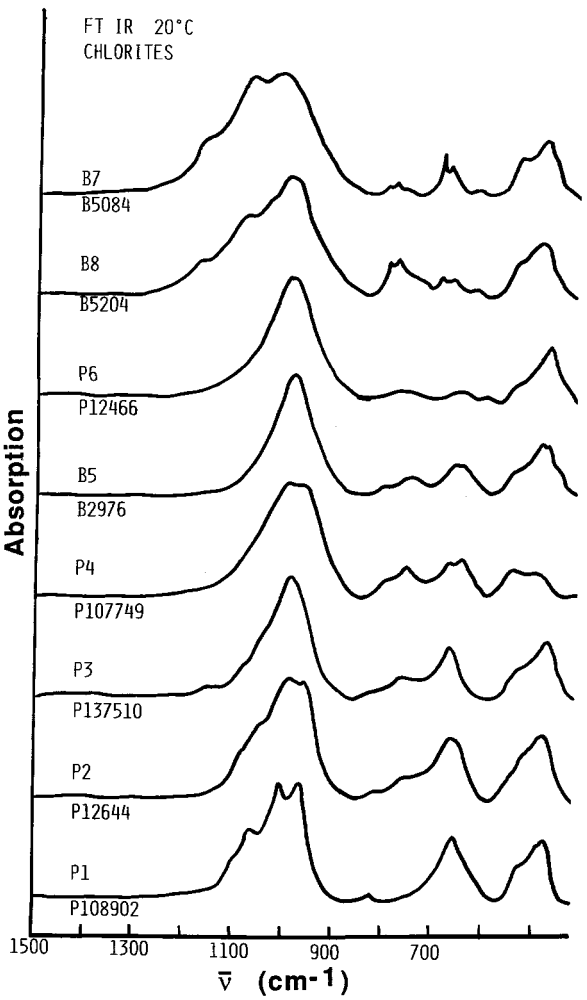

Figure 6. Infrared spectra of chlorites in the 500–1500-cm^{-1} spectral range.

creased. They were assigned to a combination of vibration of ionic and molecular groups and corresponded to skeletal modes. The peak at 350 cm^{-1} in sample P1 (Figure 8) decreased strongly in intensity with the Si substitution by Al (samples P2 and P3). In addition, the clear orientation dependence observed for sample P1 disappeared for Al-rich chlorite (samples P2 and P3). This band was assigned to internal movements of octahedral sheets. Such a band has also been found in talc (Blaha and Rosasco, 1978; Rosasco and Blaha, 1980). A weak band at about 280 cm^{-1} was assigned by Ishii *et al.* (1967) and Shirozu (1985) to tetrahedral movements with the symmetry species $E_1{}^3$. The peak at 200cm^{-1} was assigned to symmetric stretching of octahedra and showed an intensity dependence with the orientation in samples P1, P2, and P3. The intensity of this band did not depend on Al-Si substitution, but was strongly dependent on the Fe-Mg substitution. It shifted towards high frequency with an increase of Al^{VI}. This band was very weak in the IR spectra, supporting the assignment to symmetric stretching of octahedra as confirmed by the Raman spectra of talc (Acosta *et al.*, 1989). Finally, spectra recorded in the two orientations showed the existence of two bands at about 100 cm^{-1}. The peak at 105 cm^{-1} in sample P1 was assigned to octahedral movements. Its intensity with the electric field perpendicular to (001) planes, [X + Y(Z, Z)X + Y], was observed only for Mg-rich samples (P1, P2, and P3). The band was absent in the spectra of Fe-rich chlorites. The band at 130 cm^{-1}, which was well observed in samples P_3 and B_5, was assigned to vibrations of the tetrahedral sheet with $E_2{}^3$ symmetry. The frequencies of both peaks shifted towards higher values with an increase of Al and Fe.

https://doi.org/10.1346/CCMN.1991.0390508 Published online by Cambridge University Press

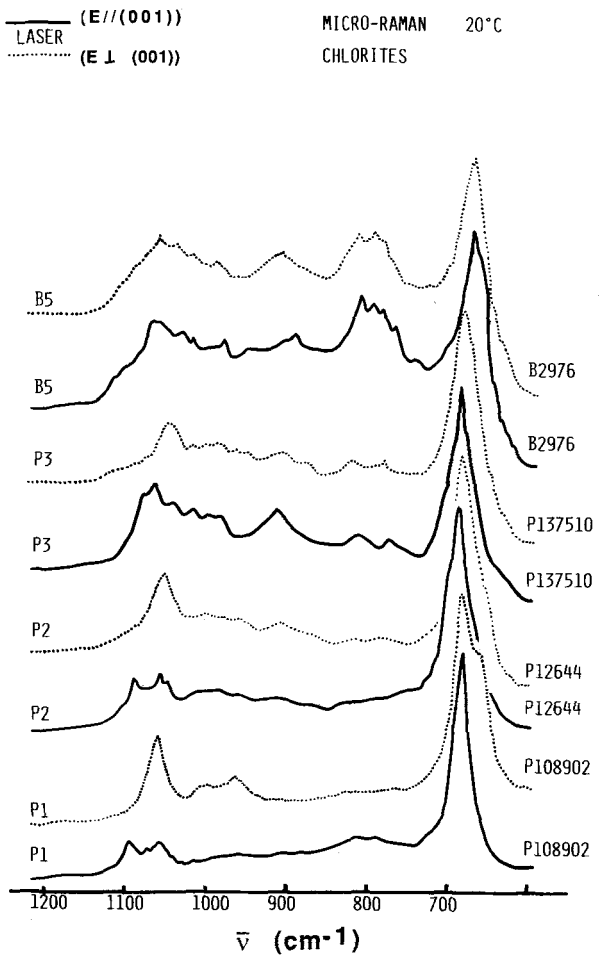

Figure 7. Raman spectra of chlorites in the 600–1200-cm^{-1} spectral range recorded in the [Z(X + Y, X + Y)Z] and [X + Y(Z, Z)X + Y] scattering geometries.

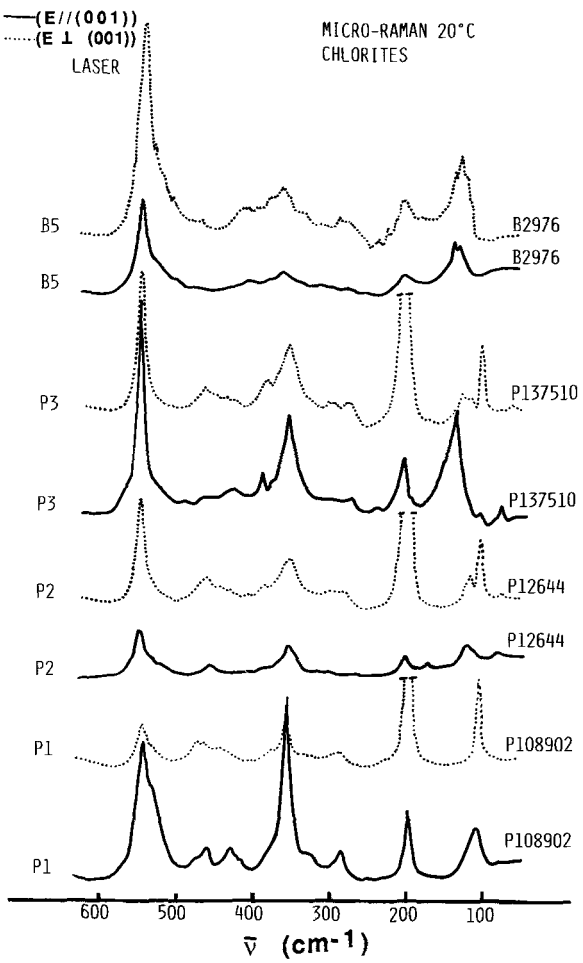

Figure 8. Low frequency Raman spectra of the studied chlorites.

SUMMARY

The wavenumber, intensity, and shape of both IR and Raman spectra of trioctahedral chlorites varied significantly with compositional changes. Thus, differences in site occupancy, which influenced the whole crystal structure have significant effects on the vibrational features, which were documented by IR and Raman spectroscopy.

The study showed that important changes occur in the 3683–3610-cm^{-1} spectral range as a function of chlorite composition; in particular, the wavenumber of the stretching band of OH groups from the 2:1 layer (band I) decreased with an increase of Fe content, at constant Al^{IV} content. In addition, the intensity was clearly dependent on the orientation of the electric field E of the laser, indicating that these OH groups were lying close to the basal planes. The more intense bands II and III were assigned following Shirozu (1980, 1985) to hydroxyl groups involved in hydrogen bonds: (SiSi)O . . . HO, with the hydrogen bonds roughly perpendicular to the basal plane, and (SiAl)O . . . HO, respectively. An increase of tetrahedral Al and octahedral Fe was accompanied by a shift towards low frequency of bands II and III, whereas an Al^{IV} was accompanied by an increase in the band III intensity and the band II widening.

In the 1300–50-cm^{-1} spectral range, IR spectra of all samples displayed four intense bands at 1090, 1050, 990, and 960 cm^{-1}, which were assigned to T–O stretching of symmetry species A_1 and E_1. The second type of bands observed in both Raman and IR spectra were located at about 650–800 cm^{-1} and were assigned to OH vibrations. The intensity of the 800-cm^{-1} Raman bands increased, and the band shifted towards higher frequency and split into several components with an increase of Fe content. The IR band at about 650 cm^{-1} decreased in intensity as Al^{IV} or Fe increased, showing its strong dependence on the composition of the interlayer octahedral sheet.

https://doi.org/10.1346/CCMN.1991.0390508 Published online by Cambridge University Press

This preliminary study of the vibrational spectroscopy of trioctahedral chlorites by Raman is a first attempt at the assessment of the compositional dependence of vibrations in phyllosilicate structures. As the chemical analysis of very thin chlorite monocrystals (<0.15 mm in thickness) is difficult by conventional methods, such as electron microprobe and XRD, both micro-IR and Raman spectroscopy will help their *in situ* characterization if samples are homogeneous. Such data will be very useful to the petrologists and mineralogists involved in the study of water-rock interactions occurring in hydrothermal or diagenetic systems.

ACKNOWLEDGMENTS

The authors thank F. A. Mumpton and an anonymous referee for very helpful reviews. The Bern and Paris museums are thanked for the samples kindly provided. Mr. J. M. Claude is acknowledged for help with the electron microprobe analysis carried out at the Service commun d'analyse de l'Université de Nancy I.

REFERENCES

Acosta, A., Alia, J. M., Prieto, A. C., and Rull, F. (1989) Caracterizacion estructural de talcos: Aplicaciones a los talcos de Charches (Granada): *Bol. Soc. Esp. Min.* **12,** 1–22.

Blaha, J. J. and Rosasco G. J. (1978) Raman microprobe spectra of individual microcrystals and fibers of talc, tremolite, and related silicate minerals: *Anal. Chem.* **50,** 892–896.

Cathelineau, M. (1988) Cation site occupancy in chlorites and illites as a function of temperature: *Clay Miner.* **23,** 471–485.

Cathelineau, M. and Nieva, D. (1985) A chlorite solid solution geothermometer. The Los Azufres (Mexico) geothermal system: *Contrib. Mineral. Petrol.* **91,** 235–244.

Chernovsky, J. V., Jr., Berman, R. G., and Bryndzia, L. T. (1988) Stability, phase relations and thermodynamic properties of chlorite and serpentine group minerals: in *Hydrous Phyllosilicates (Exclusive of Micas),* S. W. Bailey, ed., *Reviews in Mineralogy,* **19,** Mineralogical Society of America, Washington, D.C., 225–294.

Farmer, V. C. (1974) The layer silicate: in *The Infrared Spectra of Minerals,* V. C. Farmer, ed., Miner. Soc. Monograph **4,** London, 331–363.

Foster, M. D. (1962) Interpretation of the composition and a classification of the chlorites: *U.S. Geol. Surv. Prof. Paper* **41A,** 1–33.

Hayashi, H. and Oinuma, K. (1965) Relationship between infra-red absorption spectra in the region of 450–900 cm^{-1} and chemical composition of chlorite: *Amer. Mineral.* **50,** 476–483.

Hayashi, H. and Oinuma, K. (1967) Si–O absorption bands near 1000 cm^{-1} and OH absorption bands of chlorites: *Amer. Miner.* **52,** 1206–1210.

Ishii, M., Shimanouchi, T., and Nakahira, M. (1967) Far infrared absorption spectra of layer silicates: *Inorganic Chem. Acta* **1,** 387–392.

Laird, J. (1988) Chlorites: Metamorphic petrology: in *Hydrous Phyllosilicates (Exclusive of Micas),* S. W. Bailey, ed., *Reviews in Mineralogy* **19,** Mineralogical Society of America, Washington, D.C., 405–454.

Oinuma, K. and Hayashi, H. (1968) Infrared spectra of clay minerals: *J. Tokyo. Univ. Gen. Educ. (Nat. Sci.)* **9,** 67–98.

Pampuch, R. and Ptak, W. (1968) Infrared spectra of 1:1 layer silicates: *Polska. Akad. Nauk, Oddzial Krakowe, Prace Miner.* **15,** 7.

Poulet, H. and Mathieu, J. P. (1970) *Spectres de Vibration et Symétrie des Cristaux:* Gordon and Breach, Paris, 438 pp.

Prieto, A. C., Dubessy, J., Cathelineau, M., and Rull, F. (1990) Estudio y caracterizacion de cloritas trioctaedricas por espectroscopia Raman e infra-Rojo: *Bol. Soc. Esp. Min.* **13,** 25–34.

Rosasco, G. J. and Blaha, J. J. (1980) Raman microprobe spectra and vibrational mode assignments of talc: *Appl. Spectroscopy* **34,** 140–144.

Serratosa, J. M. and Vinas, J. M. (1964) Infrared investigation of the OH bands in chlorites: *Nature* **202,** 999.

Shirozu, H. (1980) Cation distribution, sheet thickness, and O–OH space in trioctahedral chlorites—An X-ray and infrared study: *Miner. J.* **10,** 14–34.

Shirozu, H. (1985) Infrared spectra of trioctahedral chlorites in relation to chemical composition: *Clay Sci.* **6,** 167–176.

Shirozu, H. and Ishida, K. (1982) Infrared study of some 7 Å and 14 Å layers: *Miner. J.* **11,** 161–171.

Shirozu, H. and Nomoi, H. (1972) Infrared spectra of trioctahedral chlorites: *Miner. J.* **6,** 464–476.

Shirozu, H., Sakasegawa, T., Katsumoto, N., and Oxaki, M. (1975) *Clay Sci.* **4,** 305–321.

Stubican, V. and Roy, R. (1961) Isomorphous substitution and infrared spectra of the layer lattice silicates. *Amer. Mineral.* **46,** 32–51.

Tuddenham, W. M. and Lyon, R. J. P. (1959) Relation of infrared spectra and chemical analysis of some chlorites and related minerals: *Analyt. Chem.* **31,** 377–380.

Vedder, W. (1964) Correlation between infrared spectrum and chemical composition of micas: *Amer. Mineral.* **49,** 736–768.

Walshe, J. L. (1986) A six-component chlorite solid solution model and the conditions of chlorite formation in hydrothermal and geothermal systems: *Econ. Geol.* **81,** 681–703.

(Received 16 August 1990; accepted 15 May 1991; Ms. 2031)